



Transcription factor KLF4 modulates microRNA-106a that targets Smad7 in gastric cancer



Meng Zhu^a, Ning Zhang^b, Shuixiang He^{a,*}

^a Department of Gastroenterology, First Affiliated Hospital of Xi'an Jiaotong University, 277 West Yanta Road, Shaanxi, Xi'an, 710061, China

^b Department of Pathology, General Hospital of Ningxia Medical University, 804 Shengli Street, Ningxia, Yinchuan, 750004, China

ARTICLE INFO

Keywords:

Gastric cancer
Invasion
KLF4
MicroRNA-106a
Smad7

ABSTRACT

Mounting evidence has revealed that microRNAs (miRNAs, miRNA) play oncogenic or anti-oncogenic roles in many cancer types. Our previous studies have found the ectopic expression of miR-106a in gastric cancer. However, its deregulation and some potential targets have not yet been fully explored. In this investigation, we identified that the upstream transcriptional factor krüppel-like factor 4 (KLF4), a novel regulator, directly bound to the promoter sequence of miR-106a and was responsible for its deregulation. Using real-time PCR and immunohistochemistry, we further verified that the expression level of KLF4 was negatively correlated with the miR-106a expression in tissue samples. Moreover, the downstream locus was also screened and small mothers against decapentaplegic 7 (Smad7) was revealed to be a direct target of miR-106a, with its 3'-UTR region complementarily bound to miR-106a and the protein expression was mediated by miR-106a in gastric cancer cells, which was confirmed by luciferase assay and Western blot. The role of KLF4-miR-106a-Smad7 in gastric cancer invasion was assessed by real-time PCR and transwell assay. The promoting effect of miR-106a on gastric cancer invasion was significantly abolished by the overexpression of KLF4. The silencing of Smad7 partially promoted the cell invasion when miR-106a was suppressed. In conclusion, we suggest that the ectopic expression of miR-106a is modulated by the upstream transcriptional factor KLF4, which influences the invasive ability of gastric cancer through the downstream target Smad7. MiR-106a should, therefore, be considered as a potential molecular phenotype in gastric cancer.

1. Introduction

Gastric cancer is the one of the most common cancer around the world although its diagnosis is, to some degree, determined at its early stages, especially in the West or developed countries. This advancement has been achieved due to a series of cancer control programs, including cancer screening programs, that have been launched in high risk areas [1]. However, gastric cancer remains the leading cause of cancer-related death in the developing countries, in which most cases are diagnosed at an advanced stage that are often accompanied by multiple metastases. Statistical estimates show that 4,292,000 new cancer cases and 2,814,000 cancer deaths in China in 2015. Gastric cancer ranks among the top five malignant tumors with the highest morbidity and mortality in China [2]. Therefore, it is a significant burden to the health system in our country. The occurrence of this severe disease is related mainly to the eating habits of Chinese. For example, the intake of smoked pickled or salted food is very common in the northwest of

China, especially in rural areas [3]. The population in these villages still uses well water/pit water. Other reasons are the widespread *Helicobacter pylori* infection and familial aggregation.

The pathogenesis of gastric cancer has always been thought to be caused by combination of internal genetic and external environmental factors [4]. For example, such factors are the abnormal regulation of many cytokines and uncontrolled growth and unceasingly increased malignant degree. MicroRNAs (miRNAs, miRNA) are small conserved ribonucleic acids produced from non-coding parts of the genome. The non-coding sequences represented by miRNAs are responsible for the control of cellular and physiological processes [5,6]. The importance of miRNAs to cancer development has been repeatedly emphasized in a great number of publications, because they are involved in multiple processes, including cell differentiation, cell growth, regulation of cell cycle, etc. [7]. It is known that miRNAs are classes of approximately 17- to 25- nucleotide non-coding molecules which regulate diverse target genes at posttranscriptional or translational level. Many conserved

Abbreviations: MiR-106a, microRNA-106a; KLF4, krüppel-like factors 4; Smad7, small mothers against decapentaplegic 7; TGF- β , transforming growth factor β

* Corresponding author.

E-mail address: hex123@126.com (S. He).

<https://doi.org/10.1016/j.prp.2019.152467>

Received 6 March 2019; Received in revised form 12 May 2019; Accepted 21 May 2019

0344-0338/ © 2019 Elsevier GmbH. All rights reserved.

miRNAs display preferentially conserved interactions with hundreds of target mRNAs, which embodies its multi-target and multi-function properties [8]. In the past decades, thousands of human genes have been identified to be miRNA targets [8,9]. In our previous study, we found that the overexpression of miR-106a influenced various biological pathways of gastric cancer. By interacting with target genes, miR-106a regulates tumor progression and metastasis in the cells. Many other studies, including ours, have so far identified several targets for miR-106a, such as TIMP2, RUNX3 and BCL2L11 [10–12]. The different downstream targets correspond to different miRNA functions, which provide positive or negative feedback to multiple cell phenotypes. Beyond that, upstream elements modulating the transcription of mature miRNAs are also important factors causing an imbalance in miR-106a in gastric cancer, which has also not been sufficiently explored. These two aspects prompted us to examine the role of miR-106a in gastric cancer invasion and study the mechanism of its deregulation in depth.

In the present study, we found that a direct transcriptional inhibitor KLF4, which is responsible for miR-106a's upstream modulation and directly targets Smad7, which participates in miR-106a's downstream regulation. In addition, the role of the signal axis of KLF4-miR-106a-Smad7 in gastric cancer is involved in the regulation of cell invasiveness, and thus, miR-106a may be regarded as a potential molecular phenotype for its oncogenic properties.

2. Materials and methods

2.1. Bioinformatics retrieval

For prediction of miRNA upstream transcriptional factor, the UCSC website (<http://genome-asia.ucsc.edu/cgi-bin/hgGateway?redirect=manual&source=genome.-ucsc.edu>) was entered to analyze the promoter sequence of hsa-miR-106a. Sequence retrieval region options (Promoter/Upstream by 2000 bases) were selected, and the miR-106a promoter sequence (> hg38_knownGene_uc004exg.1 range = chrX:134170279-134172278 5'pad = 0 3'pad = 0 strand = - repeatMasking = none) was acquired after submission. Then, the JSAPAR database (<http://jaspar.binf.ku.dk/>) CORE Vertebrata was scanned to obtain all transcriptional factors that might bind to the miR-106a promoter sequence. The following transcriptional factors were identified: HIF1A, ZEB1, ZNF354C, Myod1, KLF4, Tcf12, E2F6, E2F1, Hltf, Sox3, etc. Given that proximity of the binding site to the starting site, and the fragment length of coding sequence, we chose KLF4 as the candidate. Next, the binding site of KLF4 to miR-106a promoter was identified. The predicted site sequence was gggcgggcc or ggggtggggg with the score of 9.878 or 11.453, respectively. The two putative sites were predicted with these setting (90%) in a sequence named hg38_knownGene_uc004exg.1. For prediction of miRNA downstream mRNA targets, three types of software (TargetScan, miRanda, DIANA-T) were used to analyze and predict the potential binding genes for miR-106a.

2.2. Plasmid construction

To construct hsa-miR-106a promoter wild/mutant reporter vectors, DNA was extracted from 200 μ L of GES-1 cell suspensions with a Biospin DNA extraction kit (Bioer Technology, Hangzhou, China). The procedure included multiple elution, filtration, and centrifugation steps to obtain genome DNA. A volume of 1 μ L of DNA template was required for the polymerase chain reaction (PCR) amplification, followed by the retrieval of PCR products using 1% agarose gel electrophoresis to elute DNA. PCR product and PGL3 basic vector were digested with KpnI and XhoI (ThermoFisher Scientific, Waltham, MA, USA) and then retrieved for conjugation with T4 DNA Ligase (ThermoFisher Scientific, Waltham, MA, USA). A volume of 10 μ L of the product was transformed into 100 μ L *Escherichia coli* (*E. coli*) DH5 α competent cells, and 1 μ L bacterial solution was used as a template for PCR identification. Plasmids were extracted using Plasmid Mini Kit (Omega Bio-tek, Norcross, GA, USA) according to the instructions of the manufacturer.

After washing several times and validation, the obtained plasmids were reacted with KpnI and XhoI (ThermoFisher Scientific, Waltham, MA, USA) and identified with electrophoresis. For construction of the KLF4 and Smad7 overexpression plasmid, RNA was extracted from GES-1 cells using the TRIzol reagent. After elution, reverse transcription was conducted by RT-PCR with 10 μ g RNA used as a template and cDNA was obtained. The PCR retrieval product and pcDNA 3.0 vectors were cut out by KpnI and XhoI (ThermoFisher Scientific, Waltham, MA, USA) after the target gene had been amplified. The remaining steps were identical to the aforementioned. The primers for the Smad7 wild/mutant vectors were designed based on the Smad7 3'-UTR sequence and the psiCHECK-2 vector. RNA extraction was completed by the TRIzol method, followed by reverse transcription using a Bestar qPCR RT Kit (DBI Bioscience, Ludwigshafen, Germany). DNA was eluted by electrophoresis of PCR products. The Smad7 gene products and psiCHECK-2 vector were extracted and digested with XhoI and NotI, and linked using T4 DNA Ligase (ThermoFisher Scientific, Waltham, MA, USA). Next, transformation was performed to 100 μ L of *E. coli* DH5 α competent cells. The positive clones were selected for plasmid extraction after the bacterial solutions underwent PCR amplification and electrophoresis. After enzyme digestion appraisal to the restructuring plasmid, we submitted it to Sangon Biotech Corporation (Shanghai, China) for testing the validity of the targeted sequences. Table 1 presents a compilation of the primers sequence.

2.3. Cell culture and tissue collection

HEK293T and human immortalized gastric mucosal epithelial cell GES-1 were severally maintained in Dulbecco's Modified Eagle's Medium (DMEM, Hyclone, Logan, Utah, USA) and Roswell Park Memorial Institute 1640 (RPMI-1640, Hyclone, Logan, Utah, USA) with 10% fetal bovine serum (FBS, Gibco, California, USA), supplemented with penicillin/streptomycin in a 5% carbon dioxide/95% environment at 37 °C. Human gastric cancer cells SGC-7901 and AGS were cultured in RPMI-1640 medium using the same nutrient described above. The cell lines were purchased from the Type Culture Collection of the Chinese Academy of Sciences, Shanghai, China. Tissues were collected from General Hospital of Ningxia Medical University, where the clinical patients were subjected to surgery. Then, specimens from the stomach were extracted for experimental application after pathological diagnosis. The total number of patients included in this study was 40. Gastric cancer and paracancerous tissues were incised from each patient. For each specimen, we obtained informed consent signed by the patient and ethical ratification, approved by the local Ethics Committee.

2.4. Dual-luciferase reporter-gene assay

Dual-luciferase reporter-gene assay was used to analyze the direct effect of the upstream regulator KLF4 on miR-106a and the miR-106a's direct downstream target Smad7. For KLF4, HEK293 T cells were cultured and inoculated into 24-well plates with cell density at 8×10^5 /ml, followed by transfection with 0.8 μ g miR-106a promoter wild (WT)/mutant (MUT) reporter vectors or KLF4 overexpression (KLF4⁺) plasmid with the reagent Lipofectamine™ 2000 (Invitrogen, Carlsbad, CA, USA). The following experimental groups were studied: pmiR-106a-WT + KLF4⁺ plasmid, pmiR-106a-WT + blank plasmid, pmiR-106a-MUT + KLF4⁺ plasmid, and pmiR-106a-MUT + blank plasmid. Dual-Luciferase® Reporter Assay System was purchased from Promega Corporation with firefly luciferase (Luc) activity as the reporter gene and renilla (Rluc) luciferase as the reference gene. Upon continuous culture for 48 h, 100 μ L of passive lysis buffer was added to each of the wells to collect the cell lysate. Then, we carefully transferred up to 20 μ L of cell lysate into the luminescent plate containing 100 μ L LARII, followed by mixing twice or thrice by pipetting, without vortexing. The background value was read by a Glomax bioluminescence detector

Table 1
Primers pairs used in this study.

Name	Gene ID	Number	Accession number sequences (5'-3')	Length
MiR-106a F	406899	NC_000023.11	GGGGTACCACACCCGGAGAGGGGG	191bp
MiR-106a R			CCGCTCGAGTTTCTCAAGTCCCGCCCG	
MiR-106a Mut F			GCTCTCCACCTGCGAA <u>TTCACTACTA</u> GGAGCTGGGTCCCGC	
MiR-106a Mut R			GCGGGACCCAGCTCCTAGTATGAATTCGCAGGTGGAGAGC	
KLF4-F1	9314	NC_000009.12	GGGGTACCATGAGGCACCCACCTGGC	1440bp
KLF4-R1			CCGCTCGAGTTAAAAATGCCTCTTCATGTGTAAGG	
Smad7-F1	4092	NC_000018.10	GGGGTACCATGTTACAGACCAACAGATCTGC	1281bp
Smad7-R1			CCCTCGAGCTACCGGCTGTTGAAGATGACCT	
Smad7 F			CCGCTCGAGCTCGTATGATACTTCGACACTGTTTC	
Smad7 R			ATTTGCGGCGCACATTTTAAAAATCGTTTAAATGGAA	
Smad7-MUT-F			AAATAAAGAAAAGAT <u>CGGTCGAGCTTTAATATAAATG</u>	
Smad7-MUT-R			CATTTATATTAAAGCTCGACCGATCTTTCTTTAATTT	
KLF4 F			CGTTGAACCTCCTCGGTCTC	
KLF4 R	139bp		GACGCCTTCAGCAGCAACT	
miR-106a RT			CTCAACTGGTGTCTGGAGTTCGGCAATTCAGTTGAGTACCTGC	
miR-106a F			ACACTCCAGCTGGGAAAAGTGCTTACAGTGCA	
Smad7 F	116bp		TTCCTCCGCTGAAACAGGG	
Smad7 R			CCTCCAGTATGCCACCAC	
ALL R			CTCAACTGGTGTCTGGAG	
U6 F			CTCGCTTCGGGAGCACA	
U6 R	108353825	NC_015438.3	AACGCTTCACGAATTGCGT	
GAPDH F			2597	NC_000012.12
GAPDH R			ATGGCATGGACTGTGGTCAT	154bp

Mutant sequences are underlined.

before initiate reading for 2 s. If available, 100 μ L of the Stop & Glo® Reagent were added subsequently and briefly vortexed to mix. Further, the sample was replaced in the luminometer, and reading for 2 s was initiated. For Smad7, GES-1 was cultured to the logarithmic growth stage, and cell density was adjusted to 8×10^5 /mL. The samples were divided into the following groups: Smad7 WT + miR-106a NC, Smad7 WT + miR-106a mimic, Smad7 MUT + miR-106a NC, Smad7 MUT + miR-106a mimic. Lipofectamine™ 2000 reagent was used for co-transfection of a mixture of 0.8 μ g psiCHECK-2 Smad7 WT or MUT report plasmid vector together with 50 nM hsa-miR-106a mimic or negative control (Genepharma, Shanghai, China). Fluorescence detection was carried out following the company's instructions (Promega, Madison, WI, USA).

2.5. H&E, IHC staining and quantitative real-time PCR

Hematoxylin and eosin (H&E) and immunohistochemistry (IHC) staining were used to visualize the negative regulation of KLF4 on miR-106a in the tissue samples. A number of 40 couples of gastric cancer and paracancerous tissues (marginal gastric tissues) were subjected to pathological studies, including H&E staining and IHC staining. All tissues were fixed in formaldehyde, and the sections were paraffin-embedded. The sectioning technology with paraffin was used, and the thickness of the slices was adjusted to 4 μ m. All immunohistochemical staining procedures were performed on EnVision™ Detection Systems, Peroxidase/DAB, Rabbit/Mouse (DAKO, Glostrup, Denmark). Next, all slices were dewaxed to water, and antigen repair was carried out in a microwave oven with ethylene diamine tetraacetic acid (EDTA, pH 9.0). Blocking endogenous peroxidase by 3% hydrogen peroxide can reduce non-specific background staining. The slides were then blocked with 3% bovine serum albumin (BSA, Solarbio, Beijing, China) for 30 min at room temperature, no need to rinse. Then, the samples were stored for a night at 4 °C in a refrigerator with the primary antibody (KLF4, 1:100, Abcam, Cambridge, MA, USA). Next, in a humid chamber, second antibody (anti-rabbit) was incubated for 50 min at room temperature. Color development was detected with 3, 3'-diaminobenzidine (DAB, DAKO, Glostrup, Denmark) and counterstained with hematoxylin. The immunoreactivity for KLF4 was detected mainly in the cytoplasm or nucleus. Real-time PCR was utilized to determine the expression level of miR-106a, KLF4 and Smad7. Total RNA was then

isolated using 1 mL of RNAiso Plus (Takara, Shiga, Japan) following the manufacturer's instructions, and cDNA was synthesized by reverse transcription of 3 μ g of total RNA with a Bestar™ qPCR RT Kit (DBI, Ludwigshafen, Germany). SYBR Green real-time RT-PCR (DBI, Ludwigshafen, Germany) was employed to analyze their mRNA level. Primers sequence was shown in Table 1.

2.6. Transwell matrigel invasion assay

Transwell assay was conducted to assess the gastric cancer cells' invasive ability. For KLF4-miR-106a, SGC-7901 cells were prepared and transfected with micrON™ hsa-miR-106a-5p mimic (100 nM) and its negative control (Ribobio Biotechnology, Guangzhou, China) as well as the KLF4⁺ pcDNA vector and its basic vector with Lipofectamine™ 2000 (Invitrogen, Carlsbad, CA, USA). For miR-106a-Smad7, the cells were harvested with miR-106a inhibitor (200 nM) and its negative control together with Smad7 small interfering RNA molecule (GenePharma Biotechnology, Shanghai, China) and scrambled sequence. Briefly, 2×10^4 cells were seeded into the upper chambers (pre-coated with Matrigel, BD, San Jose, CA, USA) in serum-free RPMI-1640 medium. The lower chamber was filled with culture media containing 10% FBS as a chemo-attractant. After incubation for 24 h, the non-invaded cells on the upper surface of the chamber were scraped off with a cotton bud. Successfully translocated cells were fixed with 4% paraformaldehyde and stained with 0.1% crystal violet. The cells that passed the chambers were counted under a microscope (Olympus, Takachiho, Japan).

2.7. Western blot

Immunoblot analysis was used to evaluate the protein expression of KLF4 and Smad7 to define whether they were associated with miR-106a. Cells were broken in RIPA Lysis Buffer (Beyotime Biotechnology, Shanghai, China), and the protein concentration was quantified by a Pierce™ BCA Protein Assay Kit (ThermoFisher, Scientific, Waltham, MA, USA). The protein samples (each of 20 μ g) were separated by 10% sodium dodecyl sulfate polyacrylamide gel electrophoresis (SDS-PAGE) for approximately 1.5 h at 100 V–120 V, followed by electrophoretically transferred to PVDF membranes (Millipore, Billerica, MA, USA) at 300 mA for 150 min. The transferred PVDF membranes were washed three times with TBST. After blocking with 5% non-fat milk, the

membranes were incubated overnight at 4 °C with specific primary antibodies (KLF4, 1:1000, Abcam, Cambridge, MA, USA; Smad7, 1:500, Proteintech, Rosemont, IL, USA) and then detected with HRP-labeled goat anti-rabbit IgG (1:20,000, Boster Technology, Wuhan, China) for 40 min. A GAPDH antibody was used as control normalization. The membranes were developed using Immobilon™ Western HRP solution kit (Millipore, Billerica, MA, USA), and the protein bands were analyzed by an Image-Pro Plus 6.0 system.

2.8. Animal model

BALB/c nude mice were purchased from Vital River Experimental Animal Technology Co., Ltd (Beijing, China, Certificate SCXK 2012-0001). The mice were 4-week-old, and divided into two groups: negative control and miR-106a antagomir group (n = 10, respectively). The BGC-823 cells were transfected with miR-106a antagomir (200 nM) and collected to inject subcutaneously into abdomen of the nude mice. The tumor nodules were incised after two weeks and immunohistochemistry was used to detect the expression of KLF4.

2.9. Statistical analysis

Statistical analysis was carried out with SPSS 17.0 (Chicago, IL, USA) package. The data from cell experiments were presented as the mean ± standard deviation (SD). Comparison of two samples was analyzed by the two-tailed paired Student's *t*-test, whereas, data from multiple samples was calculated by One-Way ANOVA. The bar chart represents the correlation and difference between variables. The box plot displays the distribution features of a set of data. Statistical significance was assumed at a value of *P* < 0.05.

3. Results

3.1. Identification of KLF4 as a direct upstream transcriptional factor of miR-106a

To better understand miR-106a expression and clarify the mechanism of its deregulation, we used bioinformatics method to predict the potential transcriptional factors. From UCSC data, we obtained the promoter sequence of hsa-miR-106a. Followed by the JASPAR software, the data showed that there were several transcriptional factors that can theoretically bind to the miR-106a's promoter. We found that KLF4 was one of the transcriptional factors that can bind to the miR-106a's promoter with a high coincidence rate. In terms of the primer design, PCR amplification, and the own expression level, we finally selected KLF4 as a candidate gene. The promoter sequence of miR-106a and its potential binding site to KLF4 are illustrated in Fig. 1.

After the construction of the plasmids, we first examined the effect of pcDNA + KLF4 using real-time PCR and Western blot, and affirmed

that the plasmid can considerably promote the expression level of KLF4 both at the mRNA and protein levels. As can be seen in Fig. 2A–C, real-time PCR results revealed that the KLF4 mRNA level was significantly higher than that of the negative control group after transfection of pcDNA + KLF4 recombinant plasmid in GES-1 cells ($2^{-\Delta\Delta Ct} = 3.39 \pm 0.19, t = 18.912, P < 0.001$). Western blot analysis further confirmed that the protein level of KLF4 increased when the pcDNA + KLF4 recombinant plasmid was added to the cells (Gray value measurement: $t = -13.350, P < 0.001$). The results suggested that the constructed vector is effective and can be used in the next step. Besides, the miR-106a expression was preliminarily analyzed and confirmed its downregulation when the constructed KLF4 overexpression plasmid was used ($t = -64.494, P < 0.001, Fig. 2D$). Dual-luciferase reporter-gene assay was conducted to corroborate the direct combination of the target gene and the transcription factor. As can be observed in Fig. 2E, when the miR-106a wild-type vector was transfected with the constructed KLF4 overexpression plasmid or the blank plasmid, the relative luciferase activity of WT + KLF4 was significantly decreased compared with that of WT + NC ($t = -24.738, P < 0.001$). These differences may explain the mechanisms of the deregulation of miR-106a, which might be modulated by the transcription factor KLF4. Conversely, when the mutant type of miR-106a was transfected with the KLF4 overexpression plasmid or the blank plasmid, no significant difference was established between MUT + KLF4 and MUT + NC ($t = -1.952, P = 0.123$). The luciferase assay showed that the overexpression of KLF4 can inhibit the transcription of miR-106a, resulting in a decrease in its expression, but the effect could have been largely lost if the binding site of KLF4 to miR-106a promoter was mutated. The preliminary results confirmed the relationship of a direct combination and negative regulation between KLF4 and miR-106a.

Tissue samples were collected to further confirm the correlation between miR-106a and KLF4. As illustrated in Fig. 3A, immunohistochemical analysis in gastric cancer tissues and paracancerous tissues (non-tumor gastric epithelial tissues) yielded a result indicating that the paracancerous tissues showed high or strong positive KLF4 expression, whereas the gastric cancer tissues had lower or weak KLF4 expression. The positive rate of KLF4 was 27.5% (11/40) in the gastric cancer tissues and 77.5% (31/40) in the paracancerous tissues. The expression pattern of KLF4 in the histological specimens reflected the characteristics of the tumor suppresser gene. Table 2 summarized the correlation between KLF4 and miR-106a expression and clinicopathological parameters of gastric cancer. They were correlated with the depth of invasion, lymph node metastasis and the formation of intravascular tumor thrombus of gastric cancer. Moreover, real-time PCR was conducted to identify the negative regulation of KLF4 on miR-106a. By quantitative analysis, we found that KLF4 mRNA expression was different between gastric cancer tissues and paracancerous tissues ($\Delta Ct_{Gastric\ cancer} = 9.16 \pm 0.86, \Delta Ct_{Paracancerous\ tissues} = 8.17 \pm 0.85, 2^{-\Delta\Delta Ct} = 0.69 \pm 0.59$), suggesting that the level of KLF4 in the



B

MA0039.2	Klf4	9.878	0.904335060821089	86	95	1	ggggcgggcc
MA0039.2	Klf4	11.453	0.931094018160657	1488	1497	1	gggg!ggggg

Fig. 1. Promoter sequence of miR-106a and its potential binding site to KLF4.

(A) Retrieval of 2,000-bp sequence in the upstream promoter region of miR-106a, performed by UCSC software. The red font is a sequence that has been combined with KLF4. (B) Identification of the binding site of the transcriptional factor KLF4 to the miR-106a promoter, conducted by JASPAR software.

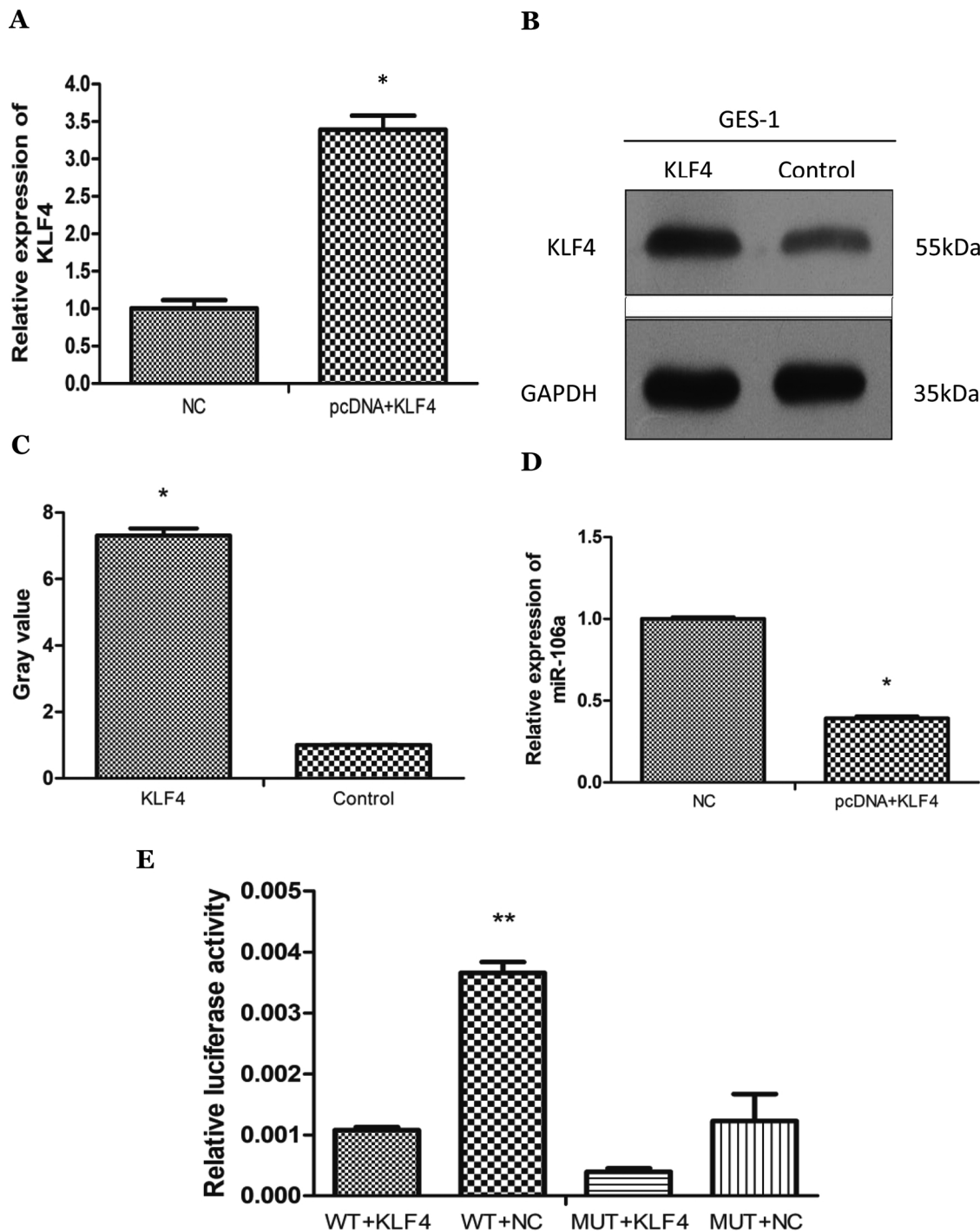


Fig. 2. Identification of KLF4 as a direct upstream transcriptional factor of miR-106a.

(A) Real-time PCR used for detection of KLF4 mRNA expression level after the transfection with pcDNA + KLF4 recombinant plasmid into GES-1 cells. The relative expression level was significantly higher in pcDNA + KLF4 group than in the NC group ($*P < 0.001$). (B) Western blot of KLF4 in GES-1 cell infected with control or KLF4-carrying plasmids. (C) The gray level of pcDNA + KLF4 increased more significantly than that in the control group ($*P < 0.001$). (D) Real-time PCR analysis of the effect of KLF4 plasmid on miR-106a expression ($*P < 0.001$). (E) Dual-luciferase reporter-gene assay of the co-transfection of miR-106a promoter with WT or MUT reporter vectors and KLF4 overexpression plasmid. Comparison of two phases, the relative luciferase activity of miR-106a-WT + KLF4 group was much lower than that of the NC group ($**P < 0.001$), however, no obvious difference was detected between the miR-106a-MUT + KLF4 group and the NC group ($P > 0.05$).

cancer tissues was lower than that in the paracancerous tissues ($t = 5.225, P < 0.001$). Conversely, miR-106a expression was at a high level in cancer tissues than that in normal tissues ($\Delta\text{Ct}_{\text{Gastric cancer}} = 3.16 \pm 0.99, \Delta\text{Ct}_{\text{Paracancerous tissues}} = 4.40 \pm 1.21, 2^{-\Delta\Delta\text{Ct}} = 3.05 \pm 2.04$). The picture was given in Fig. 3B, C. The Correlation coefficient between KLF4 and miR-106a was ($r = -0.154, P = 0.344$,

Fig. 3D). In addition, nude mice model exhibited in Fig. 4 also confirmed their negative correlation; KLF4 expressed in miR-106a antagonist group while no obvious signal could be seen in control group. Thus, to a certain extent, these results confirm the negative regulation of KLF4 in the transcriptional expression of miR-106a.

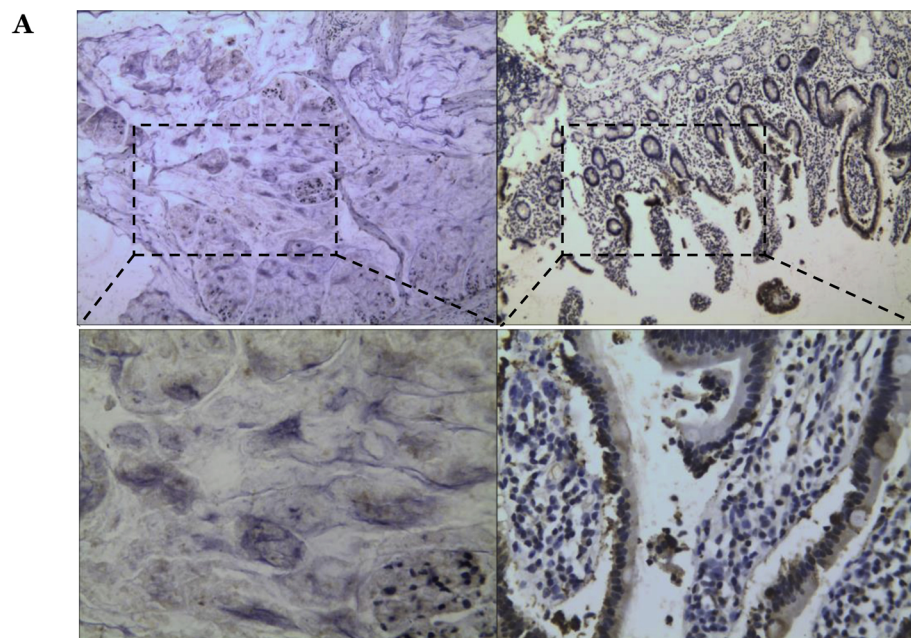
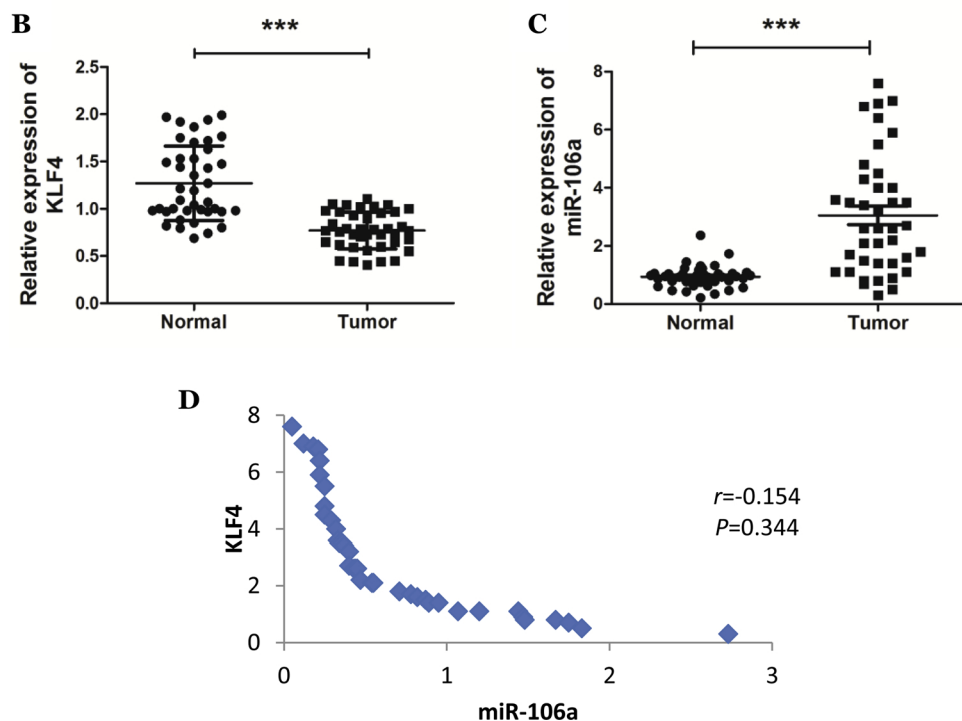


Fig. 3. Expression of KLF4 and miR-106a in gastric cancer and paracancerous tissues. (A) Immunohistochemical detection of the expression site and expression pattern of KLF4. The brown signal was mainly located in the nucleus and the cytoplasm and was distributed in the gastric mucosal epithelial cells. Left: gastric cancer; Right: paracancerous tissue; Upper, magnification $\times 100$; Lower: magnification $\times 400$. (B) Real-time PCR used for detection of the mRNA level of KLF4. The relative expression of KLF4 was obviously down-regulated in gastric cancer tissues than that in paracancerous tissues ($***P < 0.001$). (C) Real-time PCR used for detection of the miR-106a level. The relative expression of miR-106a was upregulated in gastric cancer tissues than that in paracancerous tissues ($***P < 0.001$). (D) The relative expression of KLF4 and miR-106a in gastric cancer tissues. There is a negative correlation between them. Correlation coefficient (r) = -0.154 with $P > 0.05$.



3.2. Identification of Smad7 as a direct downstream target gene of miR-106a

After we identified the direct transcriptional inhibitor for miR-106a, to further elucidate the function of miR-106a in gastric cancer progression, we considered predicting a specific target somewhat association with the transcriptional factor. We confirmed the mechanism of miR-106a deregulation at the transcriptional level, and hence, we then analyzed its post-transcriptional regulation. It is known that miRNA can target many different genes, whose function may also be different depending on the target genes changed. Using computer software analyses, we found that Smad7 had a conservative site complementary to miR-106a “seed” sequence. As can be observed in Fig. 5A–B, the Smad7 3’-UTR region had a sequence complementary with miR-106a.

Given the limited knowledge we had concerning the association of

miR-106a with Smad7, a dual-luciferase reporter-gene assay was used to ascertain the direct combination of miR-106a and Smad7. We cloned the wild-type and mutant 3’UTR of Smad7 that included the binding site of miR-106a into psiCHECK-2 vectors, named pmiR-Smad7-WT and pmiR-Smad7-MUT, respectively. Then these constructs were co-transfected with miR-106a mimic or mimic control into GES-1 cells. As depicted in Fig. 5C, when the wild type of Smad7 was transfected with miR-106a mimic and negative control, the luciferase ratio of WT/miR-106a was significantly lower (by 30.82%) than that of WT/NC ($t = 5.536, P < 0.05$). However, when the mutant type of Smad7 was transfected with miR-106a mimic and negative control, there was no significant difference between MUT/miR-106a and MUT/NC ($t = 2.392, P = 0.075$). The results indicated that Smad7 accepts the direct regulation from miR-106a. When we mutated the complementary binding sites of Smad7 to miR-106a, the fluorescence activity from the

Table 2
Correlation between KLF4 and miR-106a expression and clinicopathological parameters of gastric cancer.

Parameters	Number	miR-106a		KLF4	
		($\bar{x} \pm SD$)	P	($\bar{x} \pm SD$)	P
Sex					
Male	24	2.5017 \pm 1.27319	0.112	0.7217 \pm 0.67112	0.722
Female	16	1.9419 \pm 0.63092		0.6525 \pm 0.46318	
Age					
≥ 60	24	2.3954 \pm 1.11684	0.410	0.6842 \pm 0.51660	0.899
< 60	16	2.1013 \pm 1.05652		0.7088 \pm 0.70612	
Tumor site					
Cardia	8	2.2762 \pm 1.23978	0.309	0.6388 \pm 0.43288	0.898
Body	4	3.0675 \pm 0.34121		0.6050 \pm 0.66385	
Antrum	28	2.1654 \pm 1.08914		0.7225 \pm 0.63568	
Diameter					
> 5	10	3.0940 \pm 1.27082	0.011*	0.9310 \pm 0.78329	0.079
3-5	26	2.0815 \pm 0.91185		0.5435 \pm 0.46762	
< 3	4	1.5125 \pm 0.55835		1.0800 \pm 0.54394	
Differentiation					
Moderate	14	2.3850 \pm 0.87367	0.654	1.1436 \pm 0.85164	0.003*
Poor	26	2.2200 \pm 1.20153		0.5235 \pm 0.40474	
Infiltration depth					
Submucosa	2	0.7400 \pm 0.02828	0.023*	1.5750 \pm 0.13435	0.035*
Muscularis	6	1.6517 \pm 0.48713		0.9433 \pm 0.45129	
Serosa	32	2.4912 \pm 1.08562		0.5922 \pm 0.57725	
Lymph node					
Yes	26	2.6038 \pm 1.16514	0.008*	0.4796 \pm 0.37729	0.001*
No	14	1.6721 \pm 0.58339		1.0921 \pm 0.71523	
Tumor thrombus					
Yes	30	2.5313 \pm 1.09667	0.009*	0.5207 \pm 0.38496	0.002*
No	10	1.5170 \pm 0.63840		1.1590 \pm 0.84135	
Nerve invasion					
Yes	30	2.4900 \pm 1.10729	0.031*	0.7160 \pm 0.62399	0.689
No	10	1.6410 \pm 0.76741		0.6280 \pm 0.50259	

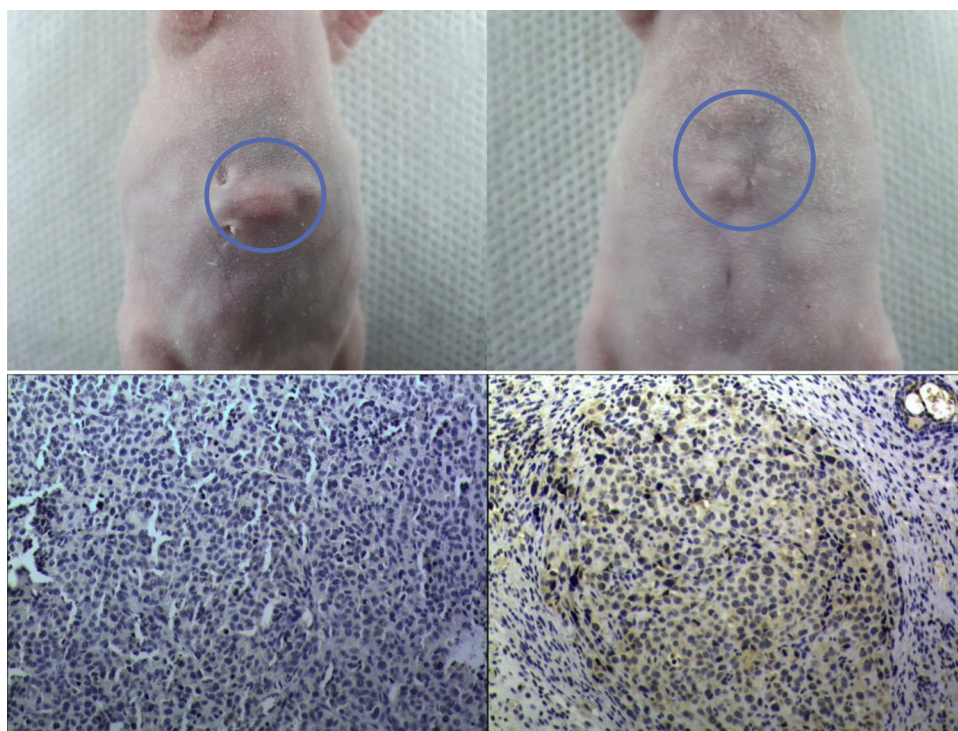


Fig. 4. Expression of KLF4 in transplanted tumor nodules.

The transplanted tumors were subcutaneously located in the abdomen of nude mice. KLF4 was dispersed in the nucleus and cytoplasm of gastric cancer cells. Left: Negative control group, Right: miR-106a antagomir group, Upper: Gross pictures. Lower: Immunohistochemical pictures. Magnification $\times 200$.

cell line was only slightly changed, and the inhibition was attenuated. This phenomenon implied that the mutant vector of Smad7 no longer accepted the regulation from miR-106a. The luciferase assay verified that Smad7 was a direct target of miR-106a.

The expression level of Smad7 was analyzed by Western blot and real-time PCR to define the post-transcriptional inhibition of miR-106a

on Smad7. The effectiveness of miR-106a mimic and inhibitor were identified first (Supplementary Fig. 1). As can be observed in Fig. 5D, E, when miR-106a mimic were added into AGS cells, the protein level of Smad7 was significantly more attenuated than that in the negative control group. Conversely, the Smad7 expression was markedly enhanced by the transient transfection of the miR-106a inhibitor. Real-

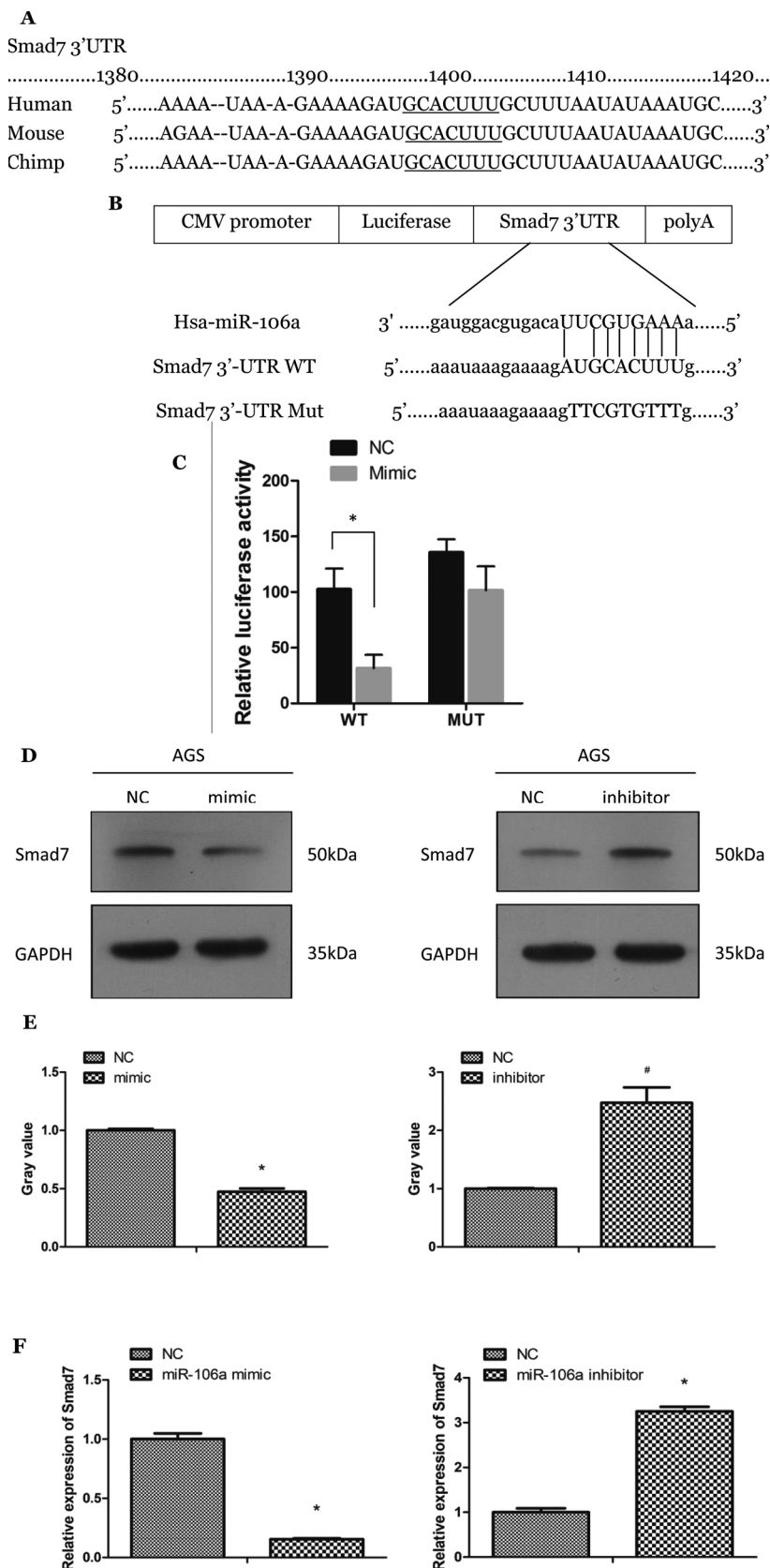


Fig. 5. MiR-106a directly targets Smad7 by binding to its 3'UTR region.
(A) Sequence conservation of target region of Smad7 by miR-106a in different species. (B) Human Smad7 gene 3'UTR region containing the wild-type or mutant miR-106a binding site was cloned into luciferase reporter vectors. (C) Luciferase assay for detecting the relative luciferase activity after co-transfection with pmir-Smad7-WT/MUT-vectors and miR-106a mimic. MiR-106a repressed Smad7 luciferase activity by targeting its wild type but not mutant 3'UTR. * $P < 0.05$. (D) Overexpression and downexpression of miR-106a in gastric cancer cells affected Smad7 protein level. (E) Gray value for detection of the Smad7 expression after treated with miR-106a mimic or inhibitor (* $P < 0.001$, # $P < 0.05$). (F) miR-106a regulates Smad7 at mRNA level. Comparing to NC group, Smad7 decreased in miR-106a mimic group or increased in miR-106a inhibitor group (* $P < 0.001$).

time PCR result in Fig. 5F showed that Smad7 decreased in miR-106a mimic group or increased in miR-106a inhibitor group ($t = 30.504$, $P < 0.001$; $t = -29.144$, $P < 0.001$, respectively).

3.3. Contribution of miR-106a to gastric cancer invasion is through the KLF4-miR-106a-Smad7 axis

After determination of the upstream transcriptional factor and

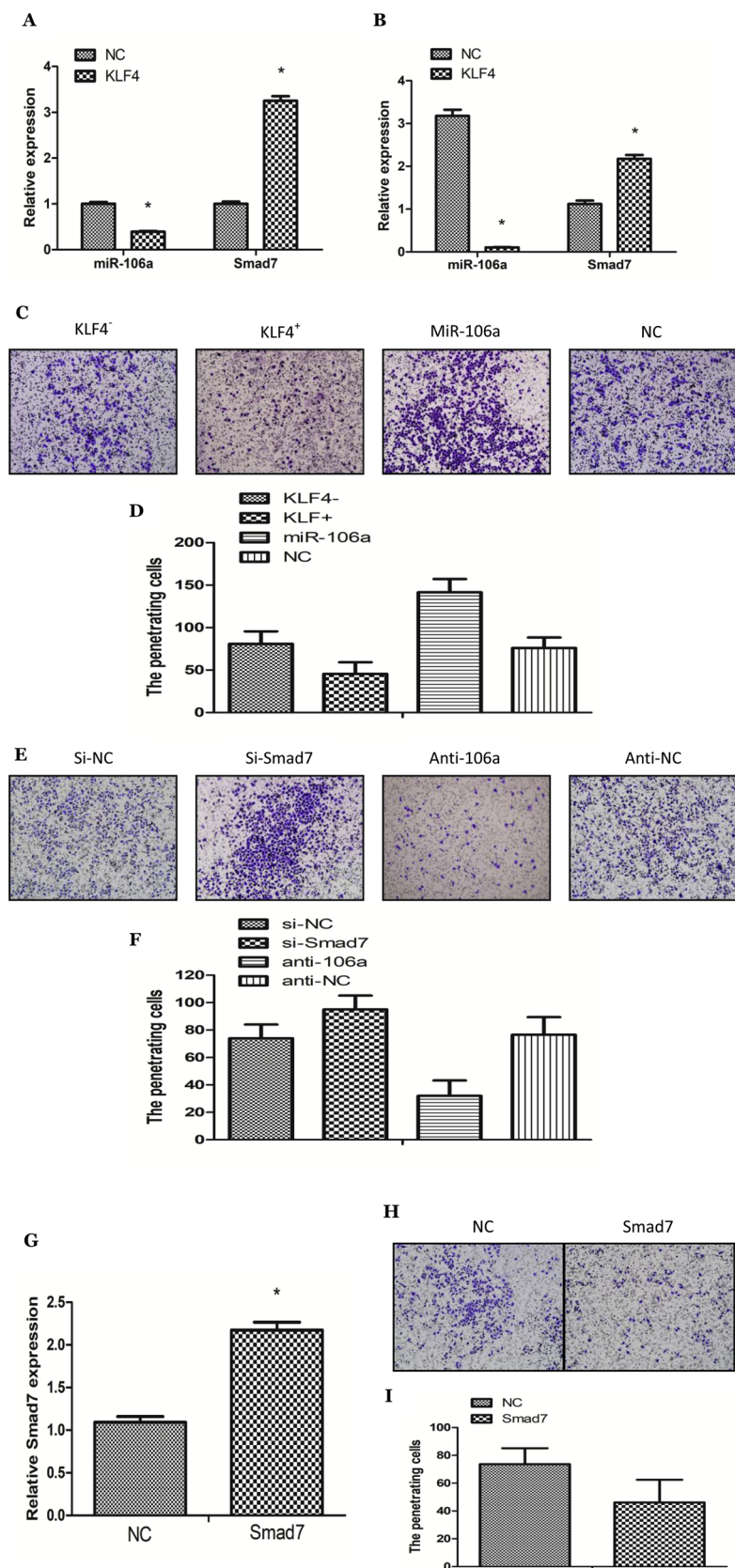


Fig. 6. KLF4-miR-106a-Smad7 axis in gastric cancer cells invasion. (A) GES-1 and (B) AGS cells were treated with KLF4 overexpression vector, and its effect on the expression of miR-106a and Smad7 were determined by real-time PCR, * $P < 0.001$. (C) and (D) SGC-7901 cells were treated with KLF4 overexpression vector (KLF4⁺) or its basic vector (KLF4⁻) together with miR-106a mimic (miR-106a) or mimic control (NC), and the effect of KLF4-miR-106a was determined with transwell invasion assay. Magnification $\times 100$. (E) and (F) Invasion assay in SGC-7901 cell treated with either Smad7 siRNA (si-Smad7) or scrambled sequence (si-NC) and miR-106a inhibitor (anti-106a) or inhibitor control (anti-NC) to assess the effect of miR-106a-Smad7. Magnification $\times 100$. (G) The overexpression plasmid of Smad7 was constructed and validated by real-time PCR, * $P < 0.001$. (H) and (I) Rescue expression was conducted in SGC-7901 cells that transfection with Smad7 overexpression plasmid, * $P < 0.001$. Magnification $\times 100$.

downstream target gene of miR-106a, to investigate whether KLF4-miR-106a-Smad7 axis was associated with cell biological behaviors, we first examine the expression changes of miR-106a and Smad7 in GES-1 and AGS cells with KLF4 overexpression. Results were shown in Fig. 6A–B,

when KLF4 was overexpressed in GES-1 cells, the miR-106a expression was suppressed at mRNA level ($t = 25.129, P < 0.001$), accompanied by the up-regulation of Smad7 ($t = -34.811, P < 0.001$). Moreover, miR-106a, which had high expression level in AGS cells, its expression

decreased after the application of KLF4 overexpression vector ($t = 37.045$, $P < 0.001$), while Smad7 increased because of the negative regulation from miR-106a ($t = -14.957$, $P < 0.001$). Together with the above experimental data, we drew the following results: KLF4 was downregulated in gastric cancer; KLF4 inhibited miR-106a at the transcriptional level; and miR-106a suppressed Smad7 at the post-transcriptional level. Because a malignant tumor progression is expressed by an increase in its ability to metastasize, we examined the invasive potential and evaluated whether the contribution of miR-106a to gastric cancer cell invasion was through the signal axis. Matrigel invasion chamber assay was performed to determine the effect of the modulation of miR-106a levels on the invasive ability of human gastric cancer cell SGC-7901. Fig. 6C–D depicted the cell invasion and cell number under the action of KLF4-miR-106a. The basic statistical analysis showed that the number of penetrating cells in the four groups was different and the data obtained were as follows: $KLF4^- = 80.90 \pm 14.70$, $KLF4^+ = 45.60 \pm 13.67$, miR-106a mimic = 141.60 ± 15.65 , mimic NC = 76.00 ± 12.40 . Statistical differences ($F = 35.364$, $P < 0.001$) was established by variance analysis. Multiple comparisons showed a statistical difference between the miR-106a mimic and mimic NC groups ($P < 0.001$; miR-106a mimic and $KLF4^+$, $P < 0.001$; miR-106a mimic and $KLF4^-$, $P < 0.001$; $KLF4^+$ and mimic NC, $P < 0.05$; $KLF4^+$ and $KLF4^-$, $P < 0.05$). However, no difference between the other two groups ($KLF4^-$ and mimic NC, $P = 0.611$) was detected. These result suggested that miR-106a can induce a stronger invasive ability in the cell. Nevertheless, this promoting effect was suppressed or weakened by the use of the KLF4 overexpression vector. The involvement of miR-106a-Smad7 in gastric cancer invasion can be seen Fig. 6E–F. The number of penetrating cells after counting under a microscope revealed a statistically significant difference among the groups ($F = 56.783$, $P < 0.001$). The following data were obtained: si-NC = 73.90 ± 10.18 , si-Smad7 = 95.00 ± 10.19 , anti-106a = 32.00 ± 11.22 , anti-NC = 76.60 ± 12.88 . Multiple comparisons showed that no significant difference was exhibited between the cell number of the si-NC and the anti-NC groups ($P = 0.592$). However, there were differences among the others (anti-106a and anti-NC, $P < 0.001$, anti-106a and si-Smad7, $P < 0.001$, anti-106a and si-NC, $P < 0.001$, si-Smad7 and anti-NC, $P < 0.05$, si-NC and si-Smad7, $P < 0.05$). Rescue experiment was shown in Fig. 6G–I, the constructed Smad7 overexpression plasmid had a capacity to decrease the invasive ability of gastric cancer cells ($t = -16.654$, $P < 0.001$). The results showed that the use of the miR-106a inhibitor decreased mature miR-106a expression levels, which led to the acquisition of enhanced expression by the target Smad7 at the post-transcriptional level, inducing a decline in the cell invasion. In contrast, the cells regained their invasive ability, and the number of perforating cells increased upon the treatment with Smad7 siRNA. Smad7, as a target gene, was also involved in the miR-106a-induced invasion. Therefore, there is a possibility that gastric cancer invasion is mediated by KLF4-miR-106a-Smad7 axis.

4. Discussion

An increasing numbers of studies revealed that the occurrence, development, and metastasis of cancer is a highly complex process, in which epithelial-derived cells acquire malignant features with high abilities of proliferation, with progressively augmented aggressiveness, caused by various factors [13,14] However, it is an inefficient and slow process in which tumor cells need to acquire a series of abilities in the presence of various oncogenic and anti-oncogenic factors [15]. Among them, miRNA is thought to be the leading factor that drives or blocks the malignant evolution of a tumor. *via* binding to many regulatory factors, miRNA inhibits the transcription of genes through post-transcriptional regulation, which results in the activation or inhibition of tumor cell invasion and metastasis. It is accepted that different types of tumors have various miRNA expression patterns, and the effect of

different miRNA on diverse types of tumors is attributed to whether they act as oncomiRs or suppressor miRs [16]. Our study focused on miR-106a, whose oncogenic roles has been confirmed by many other reports and is mainly upregulated in gastrointestinal tumors [17,18]. Its deregulation, however, is still not deeply explored, and the target gene has not yet been thoroughly investigated.

Although invasiveness is the overwhelming causes of mortality in patients with gastric cancer, the modulator and cellular determinants governing these processes remain largely unexplored [19]. MiRNA alterations is an inevitable incident in the progression of cancer and may be tightly linked to cancer invasiveness [20]. To investigate the deregulation of miR-106a in gastric cancer and its possible role, transcriptional factors able to bind to miR-106a' promoter sequences were examined, and several candidates were obtained. For selection of a transcriptional factor, it is important to take into consideration the amplification facilitation and expression levels. Recently, krüppel-like factors (KLFs) have been reported to be critically involved in both normal development and carcinogenesis. The KLFs family consists of at least sixteen different members, seven of which are the most important: erythroid KLF1, lung KLF2, basic KLF3, gut KLF4, intestinal KLF5, core promoter element-binding protein KLF6, and ubiquitous KLF7 [21]. Human KLF4 gene (gut-enriched KLF4) was first identified from human umbilical vein endothelial cell cDNA library in 1998 [22]. KLF4 is predominantly expressed in epithelial cells of the gastrointestinal tract and may be an important tumor suppresses gene, which prompts us to choose it as a potential locus. From our results, the expression of KLF4 in gastric cancer tissues was lower than that in paracancerous tissues, and the positive signals of KLF4 were mainly located in the normal gastric epithelial cells. The expression pattern of KLF4 was inversely correlated with miR-106a and could significantly attenuate gastric cancer cell invasive abilities. Therefore, combined with the analysis of the binding site of KLF4 and miR-106a promoter, the low expression of KLF4 in gastric cancer may contribute to the stimulated expression of miR-106a, and this negative regulation may play a pivotal role in gastric cancer invasion.

As a factor involved in the posttranscriptional gene regulatory mechanism, miRNA most likely participates in a wide range of life processes which include cell signal transduction [20]. The downstream target genes of miR-106a, which may be involved in gastric cancer invasion, also need to be identified. Through software analysis, small mothers against decapentaplegic (Smad) family have become an object due to its multiple roles in tumors. Smad proteins are first identified during mutational screening for the decapentaplegic gene that is responsible for the formation of *Drosophila* wings [23]. Smads are a family of signal transduction molecules in the transforming growth factor β (TGF- β) ligand pathways that have been implicated in several aspects of pathogenesis of inflammations and cancer. It is noteworthy that Smad proteins have been found to be involved in a series of potential carcinogenic mechanisms, such as gene transcription, cell differentiation and epigenetic changes [24]. Smad7 is considered to be an inhibitor of the TGF- β signal and is known to negatively regulate the TGF- β signal transduction activity due to its ability to antagonize the signal pathway by inhibition of the substrate phosphorylation [25–27]. Although Smad7 plays an important role in the progression of many malignant tumors, how the factor influences the concrete steps of gastric cancer remains unclear. Some literatures reported that Smad7 was low expressed in gastric cancer tissues and cells, and could be used as a direct target of miR-21 to participate in the regulation of proliferation, migration and apoptosis of gastric cancer cells [28]. Investigation of gastric adenocarcinoma tumor samples showed that Smad7 has lower expression level (33.1%) and significantly correlated with duration of disease-free survival [29]. Our results suggested that the post-transcriptional inhibition of Smad7 by miR-106a enhanced the invasive abilities of gastric cancer cells. Based on the mediation of TGF- β signal by Smad7 and the influence of the miR-106a-Smad7 pathway on gastric cancer invasion, we speculated that TGF- β signal might be mediated by

miR-106a-Smad7. TGF- β signal, on the one hand, acts as a potent driver of cancer through the induction of epithelial-mesenchymal transition (EMT), neo-angiogenesis, cancer progression, and metastasis [30,31]. On the other hand, TGF- β induced pathway has a closely relationship with miRNA pathway. Previous studies have shown that the TGF- β pathway includes the miRNA pathway as an important component of its downstream signaling cascades [32,33]. In our study, miR-106a is known to have an enhanced expression level in gastric cancer, induced by KLF4. The assumption is that in highly malignant tumors, with the overexpression of miR-106a, Smad7 is suppressed, the inhibition to the TGF- β signal is weakened and signal is enhanced, EMT transition is promoted and the cells obtain high invasive ability. Our result is in consistent with another report that the miR-106b-25 cluster induces EMT of human breast cancer is through targeting Smad7 and then activating TGF- β signal [34].

In addition, it should be noted that KLF family also play an important role in process of TGF- β signal transduction. KLF4 itself was found to be regulated by the TGF- β signal [35]. Based on the findings of previously published studies along those of our own research, we suggest that miR-106a may act as a bridge between KLF4 and Smad7.

Taken together, our research was focused on miR-106a, and we discussed its upstream and downstream regulatory mechanisms. From the upstream perspective, as a direct transcriptional inhibitor, KLF4 is negatively correlated with miR-106a. From downstream perspective, as a direct target, Smad7 is inversely associated with miR-106a. The signal axis of KLF4-miR-106a-smad7 is involved in the regulation of the invasive ability of gastric cancer.

Declaration of interest

No potential conflicts of interest were disclosed.

Acknowledgments

This work was supported by National Natural Science Foundation of China (grant number 81802416), China Postdoctoral Science Foundation (grant number 2018M633529), the Ningxia Natural Science Foundation (grant number NZ16148, NZ16276), and Outstanding Young Teachers Development Foundation of Ningxia Higher Education Institutions (grant number NGY2016123).

Appendix A. Supplementary data

Supplementary material related to this article can be found, in the online version, at doi:<https://doi.org/10.1016/j.prp.2019.152467>.

References

- [1] M. Venerito, G. Nardone, M. Selgrad, T. Rokkas, P. Malfertheiner, Gastric cancer—epidemiologic and clinical aspects, *Helicobacter* 19 (Suppl. 1) (2014) 32–37.
- [2] Chen, R. Zheng, P.D. Baade, S. Zhang, H. Zeng, F. Bray, A. Jemal, X.Q. Yu, J. He, Cancer statistics in China, 2015, *CA Cancer J. Clin.* 66 (2016) 115–132.
- [3] Chen, K. Sun, R. Zheng, H. Zeng, S. Zhang, C. Xia, Z. Yang, H. Li, X. Zou, J. He, Cancer incidence and mortality in China, 2014, *Chin. J. Cancer Res.* 30 (2018) 1–12.
- [4] P. Karimi, F. Islami, S. Anandasabapathy, N.D. Freedman, F. Kamangar, Gastric cancer: descriptive epidemiology, risk factors, screening, and prevention, *Cancer epidemiology, biomarkers & prevention, Cancer Epidemiol. Biomark. Prev.* 23 (2014) 700–713.
- [5] Y. Tutar, miRNA and cancer; computational and experimental approaches, *Curr. Pharm. Biotechnol.* 15 (2014) 429.
- [6] R.P. Alexander, G. Fang, J. Rozowsky, M. Snyder, M.B. Gerstein, Annotating non-coding regions of the genome, *Nat. Rev. Genet.* 11 (2010) 559–571.
- [7] D.P. Bartel, MicroRNAs: target recognition and regulatory functions, *Cell* 136 (2009) 215–233.
- [8] R.C. Friedman, K.K. Farh, C.B. Burge, D.P. Bartel, Most mammalian mRNAs are conserved targets of microRNAs, *Genome Res.* 19 (2009) 92–105.
- [9] J. Hausser, M. Zavolan, Identification and consequences of miRNA-target interactions—beyond repression of gene expression, *Nat. Rev. Genet.* 15 (2014) 599–612.
- [10] M. Zhu, N. Zhang, S. He, Y. Lui, G. Lu, L. Zhao, MicroRNA-106a targets TIMP2 to regulate invasion and metastasis of gastric cancer, *FEBS Lett.* 588 (2014) 600–607.
- [11] Zhang, Q. Lu, X. Cai, MicroRNA-106a induces multidrug resistance in gastric cancer by targeting RUNX3, *FEBS Lett.* 587 (2013) 3069–3075.
- [12] W. Tang, J. Li, H. Liu, F. Zhou, M. Liu, MiR-106a promotes tumor growth, migration, and invasion by targeting BCL2L11 in human endometrial adenocarcinoma, *Am. J. Transl. Res.* 9 (2017) 4984–4993.
- [13] S.A. Eccles, D.R. Welch, Metastasis: recent discoveries and novel treatment strategies, *Lancet* 369 (2007) 1742–1757.
- [14] G.P. Gupta, J. Massague, Cancer metastasis: building a framework, *Cell* 127 (2006) 679–695.
- [15] D. Hanahan, R.A. Weinberg, The hallmarks of cancer, *Cell* 100 (2000) 57–70.
- [16] W. Lou, J. Liu, Y. Gao, G. Zhong, D. Chen, J. Shen, C. Bao, L. Xu, J. Pan, J. Cheng, B. Ding, W. Fan, MicroRNAs in cancer metastasis and angiogenesis, *Oncotarget* 8 (2017) 115787–115802.
- [17] P. Li, Q. Xu, D. Zhang, X. Li, L. Han, J. Lei, W. Duan, Q. Ma, Z. Wu, Z. Wang, Upregulated miR-106a plays an oncogenic role in pancreatic cancer, *FEBS Lett.* 588 (2014) 705–712.
- [18] Z. Liu, E. Gersbach, X. Zhang, X. Xu, R. Dong, P. Lee, J. Liu, B. Kong, C. Shao, J.J. Wei, miR-106a represses the Rb tumor suppressor p130 to regulate cellular proliferation and differentiation in high-grade serous ovarian carcinoma, *Mol. Cancer Res.* 11 (2013) 1314–1325.
- [19] G. Di Leva, M. Garofalo, C.M. Croce, MicroRNAs in cancer, *Annu. Rev. Pathol.* 9 (2014) 287–314.
- [20] G.A. Calin, C.M. Croce, MicroRNA signatures in human cancers, *Nat. Rev. Cancer* 6 (2006) 857–866.
- [21] D. Wei, M. Kanai, S. Huang, K. Xie, Emerging role of KLF4 in human gastrointestinal cancer, *Carcinogenesis* 27 (2006) 23–31.
- [22] S.F. Yet, M.M. McA'Nulty, S.C. Folta, H.W. Yen, M. Yoshizumi, C.M. Hsieh, M.D. Layne, M.T. Chin, H. Wang, M.A. Perrella, M.K. Jain, M.E. Lee, E.Z.F. Human, A Kruppel-like zinc finger protein, is expressed in vascular endothelial cells and contains transcriptional activation and repression domains, *J. Biol. Chem.* 273 (1998) 1026–1031.
- [23] J.J. Sekelsky, S.J. Newfeld, L.A. Raftery, E.H. Chartoff, W.M. Gelbart, Genetic characterization and cloning of mothers against dpp, a gene required for decapentaplegic function in *Drosophila melanogaster*, *Genetics* 139 (1995) 1347–1358.
- [24] P. Chandrasinghe, B. Cereser, M. Moorghen, I. Al Bakir, N. Tabassum, A. Hart, J. Stebbing, J. Warusavitarne, Role of SMAD proteins in colitis-associated cancer: from known to the unknown, *Oncogene* 37 (2018) 1–7.
- [25] E. Troncone, I. Marafini, C. Stolfi, G. Monteleone, Transforming growth factor-beta1/Smad7 in intestinal immunity, inflammation, and cancer, *Front. Immunol.* 9 (2018) 1407.
- [26] Zhang, Z. Yu, Q. Xiao, X. Sun, Z. Zhu, J. Zhang, H. Xu, M. Wei, M. Sun, Expression of BAMB1 and its combination with Smad7 correlates with tumor invasion and poor prognosis in gastric cancer, *Tumour Biol.* 35 (2014) 7047–7056.
- [27] Zhang, T. Fei, L. Zhang, R. Zhang, F. Chen, Y. Ning, Y. Han, X.H. Feng, A. Meng, Y.G. Chen, Smad7 antagonizes transforming growth factor beta signaling in the nucleus by interfering with functional Smad-DNA complex formation, *Mol. Cell. Biol.* 27 (2007) 4488–4499.
- [28] Y. Jiang, M. Zhang, T. Guo, C. Yang, C. Zhang, J. Hao, MicroRNA-21-5p promotes proliferation of gastric cancer cells through targeting SMAD7, *Oncotarget* 11 (2018) 4901–4911.
- [29] A. Zizi-Sermpetzoglou, D. Myoteri, E. Arkoumani, M. Voultsos, A. Marinis, A study of Smad4 and Smad7 expression in surgically resected samples of gastric adenocarcinoma and their correlation with clinicopathological parameters and patient survival, *J. BUON* 19 (2014) 221–227.
- [30] Y. Katsuno, S. Lamouille, R. Derynck, TGF- β signaling and epithelial-mesenchymal transition in cancer progression, *Curr. Opin. Oncol.* 25 (2013) 76–84.
- [31] J. Luo, X.Q. Chen, P. Li, The role of TGF- β and its receptors in gastrointestinal cancers, *Transl. Oncol.* 12 (2018) 475–484.
- [32] H.I. Suzuki, MicroRNA control of TGF- β signaling, *Int. J. Mol. Sci.* 19 (2018) E1901.
- [33] R. Moradi-Marjaneh, M. Khazaei, G.A. Ferns, S.H. Aghaee-Bakhtiari, The Role of TGF- β signaling regulatory microRNAs in the pathogenesis of colorectal cancer, *Curr. Pharm. Des.* 24 (2019) 4611–4618.
- [34] A.L. Smith, R. Iwanaga, D.J. Drasin, D.S. Micalizzi, R.L. Vartuli, A.C. Tan, H.L. Ford, The miR-106b-25 cluster targets Smad7, activates TGF- β signaling, and induces EMT and tumor initiating cell characteristics downstream of Six1 in human breast cancer, *Oncogene* 31 (2012) 5162–5171.
- [35] Li, M. Han, M. Bernier, B. Zheng, S.G. Sun, M. Su, R. Zhang, J.R. Fu, J.K. Wen, Kruppel-like factor 4 promotes differentiation by transforming growth factor-beta receptor-mediated Smad and p38 MAPK signaling in vascular smooth muscle cells, *J. Biol. Chem.* 285 (2010) 17846–17856.